

RSC Advances



This is an *Accepted Manuscript*, which has been through the Royal Society of Chemistry peer review process and has been accepted for publication.

Accepted Manuscripts are published online shortly after acceptance, before technical editing, formatting and proof reading. Using this free service, authors can make their results available to the community, in citable form, before we publish the edited article. This *Accepted Manuscript* will be replaced by the edited, formatted and paginated article as soon as this is available.

You can find more information about *Accepted Manuscripts* in the [Information for Authors](#).

Please note that technical editing may introduce minor changes to the text and/or graphics, which may alter content. The journal's standard [Terms & Conditions](#) and the [Ethical guidelines](#) still apply. In no event shall the Royal Society of Chemistry be held responsible for any errors or omissions in this *Accepted Manuscript* or any consequences arising from the use of any information it contains.



Journal Name

ARTICLE

Hybridization of graphene sheets with polyethylene terephthalate through the process of in-situ polymerization aided by ultrasound

Pablo González Morones,* Salvador Fernández Tavizón,* Ernesto Hernández Hernández, Carlos Alberto Gallardo Vega and Arxel De León Santillán

Received 00th January 20xx,
Accepted 00th January 20xx

DOI: 10.1039/x0xx00000x

www.rsc.org/

A new methodology to prepare hybrid graphene-polyethyleneterephthalate nanocomposites by ultrasonication is reported. The hybrids were synthesized by in-situ polymerization of a mixture of bis(2-hydroxyethyl) terephthalate (BHET) monomer and graphite oxide (GO) at 200°C, in bulk. The hybrids were analyzed by Thermogravimetry (TGA), Fourier Transform Infrared Spectroscopy (FTIR), Raman spectroscopy, Transmission Electron Microscopy (TEM) and X Ray Diffraction (XRD). The analyses show the grafting of PET oligomers to exfoliated graphene sheets. The results suggest that during the polymerization process exfoliation of the GO and reaction of BHET with its oxygen containing functional groups takes place. The procedure offers a new alternative to manufacture hybrid graphene-PET nanocomposites that can be used in diverse applications.

INTRODUCTION

In order to take advantage of graphene's well known photo-electronic¹ properties, thermal and electrical conductivity², mechanical strength³ and others, a great deal of research has been devoted to develop polymer nanocomposites to manufacture optical devices⁴, gas sensors⁵, controlled release carriers⁶, capacitors⁷, solar cells⁸, batteries⁹ among many possible examples. It has been found that to advantageously use these nanocomposites it is important that the graphene layers are well dispersed in the polymer matrix in order to transfer its characteristics to the embedding polymer, to this end, it is necessary to substantially increase the compatibility between the components. One way to achieve it is to chemically join the polymer to the graphene so that the material is embedded from the start into a substrate well matched to facilitate the required dispersion. As part of an ongoing project to enhance the mechanical and electrical properties of polyethylene terephthalate (PET) based on graphene composites, we explored methods to enhance the dispersion of graphene into the polymer seeking to avoid the carbon material to agglomerate during the preparation process. We envisioned that the use of a grafting from graphite oxide (GO) covalent *in-situ* polymerization of BHET

would give rise to grafted PET oligomers on the graphene's surface, leading to polymeric hybrid nanocomposites (PHNCs) compatible with the virgin resin, easily dispersing in it without restacking. PHNCs is a class II of polymer nanocomposites where the phases are linked together through covalent or ionic bonds.¹⁰⁻¹²

Compared to non-hybridized graphene nanocomposites, it has been shown that PHNCs have better mechanical properties such as tensile strength¹³ and Young modulus¹⁴, as well as higher electrical conductivity¹⁵ and bio-compatibility.^{16, 17} As a result, a large number of PHNCs preparation processes have been developed based in 'Grafting to' and 'Grafting from' protocols.^{18,19, 20} In the first method hybridization is achieved by joining previously synthesized polymers to GO or modified GO, commonly by esterification, amide formation or 'click' chemistry,^{14,15-17}. The 'Grafting from' polymerization procedure is based on the reaction of the carboxyl, hydroxyl or epoxide groups present on the GO with appropriately functionalized moieties. ATRP, RAFT, free radical polymerization or ring opening polymerization are often used^{15,13, 18,21-23}

Recently several more environmentally friendly 'green methods' have been developed to prepare composites; as an example, Luca-Valentini et al modified graphene sheets by treating them with a CF₄ radiofrequency plasma, no solvents were used and shorter treatment times were required.²⁴ Similar 'green' protocols have been developed to cross link and cure graphene containing polymers and in sol gel synthesis. In the first case the crosslinking is achieved in a short time with a cross-linking speed of 10 mm/min in the

Centro de Investigación en Química Aplicada, Boulevard Enrique Reyna 140, 25294 Saltillo, Coahuila, México. E-mail: pablo.gonzalez@ciqa.edu.mx; salvador.fernandez@ciqa.edu.mx; Tel. +52 844 4389830.

* Footnotes relating to the title and/or authors should appear here. Electronic Supplementary Information (ESI) available: [details of any supplementary information available should be included here]. See DOI: 10.1039/x0xx00000x

absence of solvents.^{25, 26} The sol-gel process is done in aqueous solution without organic solvents.²⁷ Ultrasonication (US) is applied to disperse and exfoliate the materials in most of the processes that use solvents; however US has not been used to promote the covalent bond formation between the polymer and GO.

We report a new graphene-PET nanocomposite hybrid synthesis process based on the use of ultrasound irradiation to *in-situ* polymerize and graft bis(2-hydroxyethyl) terephthalate (BHET) to GO to obtain PET oligomers attached to graphene. The method is solvent-free, takes place in a short time (10 min) and is carried out at 200°C, a substantially lower temperature than the 240 and 280°C temperature reported to polymerize BHET monomer.^{28, 29} Exfoliated and covalently PET grafted graphene sheets can be obtained through this method.

EXPERIMENTAL PART

Materials

Graphite oxide was prepared using the method reported by Ji Chen et al.³⁰ Reagent grade BHET, 95% purity, from Sigma Aldrich was used as purchased.

PET-Graphene hybrid nanocomposites synthesis

In a typical experiment, the PHNCs were synthesized from 3.6 g of BHET and 0.4 g of GO, a 10% weight ratio of the latter. Both starting materials were heated to 200 °C while being magnetically stirred at 150 rpm on a hot plate. After reaching 200 °C the mixture was ultrasonicated for 10 min using a Cole-Parmer CPX750 model Ultrasonic Processor, at 20 kHz frequency and 20% amplitude; the thus obtained material is referred as PET-G. To separate the grafted material from non-grafted PET oligomers formed during the reaction, 2 g of the resulting solid were magnetically stirred for three hours in 50 mL of chloroform; the resulting suspension was sonicated 10 min with the a Cole-Parmer CPX750 model Ultrasonic Processor, at 20 kHz frequency and 40% amplitude. It was then filtered through a 200 nm pore membrane and the separated solid subjected five additional times to the same purification process; the obtained solid was dried in a oven at 80 °C and 0.04 MPa for 8 h; this purified hybrid is referred as G-PETH.

Characterization

In the product's characterization by infrared spectrometry a Transform Infrared (FTIR) a Thermo Nicolet spectrometer model MAGNA 550 was used, employing an attenuated total reflectance (ATR) technique using 100 sample scans at a 16 cm⁻¹ resolution. Raman spectroscopy analysis was carried out on a Micro-Raman Horiba XploRA equipment in a frequency range of 1000 to 400 cm⁻¹ with a 532 nm laser. A TA Instruments TA-Q500 model was used for the samples thermogravimetric analysis (TGA); the materials were subjected to 10 °C/min heating in a 25 to 600°C temperature range,

under a nitrogen atmosphere (50 mL/min). X Ray diffractometry was done in a Siemens D5000 diffractometer equipped with a Cu 1.54 Å irradiation source; the samples were scanned from 5 to 40 ° at 2θ, scan step 0.06 ° at 3 s. The molecular weight of the PET side product was determined by gel permeation chromatography (GPC) with a low temperature Waters Alliance GPC 2695 chromatographer with a 35°C operation temperature, using an UV Waters 2998 detector set at 248 nm; HFIP and chloroform HPLC grade were used as diluents employing a column capable of detecting molecular weights in the range of 580 to 2,700,000 g/mol based on a Polystyrene standard. The nanocomposite morphology was observed using a JEOL® Field Emission Scanning Electron Microscope (FE-SEM) model JSM-74101F and obtaining images by Transmission Electron Microscopy (TEM) with a TITAN® 300 KV microscope model JSM-74101F. Samples analyzed by FE-SEM and TEM were prepared from the graphene grafted PET (G-PETH) sample, once it was separated from the first product PET-G with the aid of chloroform, as indicated in the last section. This sample was placed into chloroform in a ratio of 0.01mg/1mL and sonicated in an ultrasound bath for 15 min to promote the sample's dispersion in the solvent. Then a copper Lacey carbon grid was used to support the sample.

Assesment of the samples' surface morphological characteristics was carried out by atomic force microscopy (AFM) on a DimensionTM 3100 from Digital Instruments with Pt-coated Si tip with 15 nm nominal radius model: OSCM-PTBruker, the images were obtained in the tapping mode at a scanning rate of 1.0 Hz during 256 lines. The morphological images shows surface roughness (Rq), given by the root mean square average (RMS) of height deviation, is taken from the data plane. The profile steps were obtained by analysis from the surface of the samples using the Nanoscope IIIa software available in the microscope.

Scheme 1 depicts the synthesis of the PET-G nanocomposite hybrid; a mixture of GO and BHET is heated with mixing to a 200 °C temperature at which time it is US irradiated. The initial mixture forms a brown colored suspension (GO original color), which shortly after starting the US treatment starts the liberation of gas and within 5 min develops a black color; bubbling continues for an additional 3 min and at this stage the suspension is completely black. The observed color change and the liberation of gas suggests the decomposition of GO with the expulsion of CO₂ and water and probably its concomitant functionalization to form PET oligomers with the removal of ethylene glycol from the reaction mixture. The suspension's homogeneity and uniform black coloration is indicative of the oxide's reduction to give raise to graphene derivatives and their possible exfoliation into mono or few layer materials.

RESULTS AND DISCUSION

We carried out an FTIR characterization to confirm the synthesis of the terephthalate NCPH, in Figure 1 we show the GO, BHET, PET-G, and PET respective IRs, the latter obtained from the equipment's library and included for comparative purposes. The PET-G infrared shows signals at 1725 cm^{-1} , 1267 cm^{-1} and 1099 cm^{-1} , characteristic of PET's signals of C=O, C-C-O and O-C-C respectively; as observed, the infrared spectra of PET-G and PET are very similar. It can be seen that PET-G lacks signals in the range of $3500\text{ a } 3200\text{ cm}^{-1}$ characteristic of hydroxyl groups of GO (3328 cm^{-1}) and BHET (3450 cm^{-1}). In the case of GO, the signal's absence suggest its reduction under the reaction conditions and the possible formation of covalent bonds with BHET while it is also indicative of BHET's reaction to either form PET polymers or of its grafting to the GO with the subsequent formation of oligomers. Taken together they indicate that we were able to prepare PHNCs under the reaction conditions.

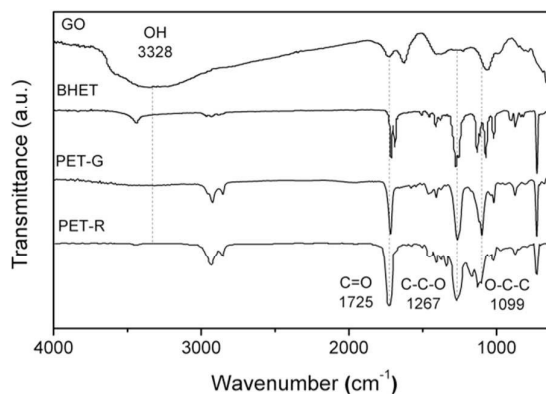
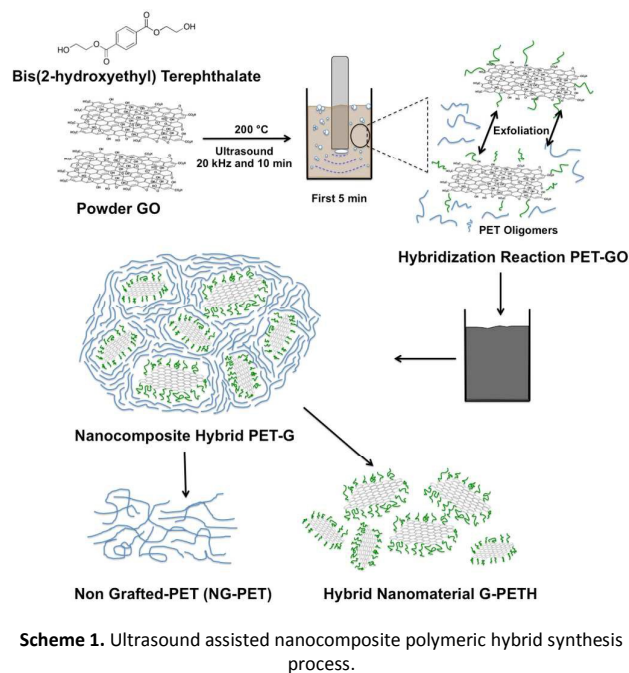


Figure 1. FTIR spectra of starting materials GO, BHET, the PHNCs PET-G product and a PET reference IR.

To determine whether GO was exfoliated during the NCPHs preparation X Ray diffractograms of the nanocomposite were obtained, these are shown in Figure 2. We observe that GO's characteristic diffraction at $2\theta = 11.1$ corresponding to the (002) reflection peak^{29, 31, 32} is absent in the sample's diffractogram. The PET-G diffractogram displays an amorphous peak centered at $2\theta = 23.8^\circ$ spread from at $2\theta=5$ to 35° characteristic of amorphous low-weight PET.^{33, 34} However it shows no signal of GO indicating the material to be absent in the sample and probably exfoliated in the nanocomposite. It is likely that the exfoliation resulted from the US energy applied during treatment. It is worth noting that no evident graphite's (002) signal at $2\theta = 26.7^\circ$ can be seen in the product in spite of its high carbon content, determined to be above 50wt% by TGA.

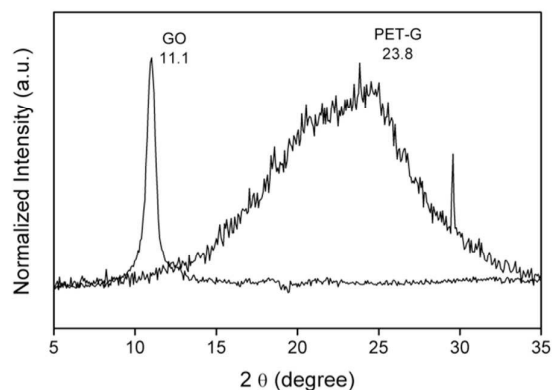


Figure 2. GO and PET-G X ray diffractograms.

Parallel to the reaction of BHET with GO to yield PET-G, polymerization into non-grafted PET (NG-PET) takes place under the reaction conditions. The soluble polymer was separated from the resulting mixture and its weight determined to be 823.3 g/mol by GPC. In Figure 3 we compare the IR-ATR of non grafted PET (NG-PET) with that of the

isolated grafted product PET-G; while in the latter the characteristic PET signals can be observed at 1725 cm^{-1} (C=O), 1267 cm^{-1} (C-C-O) and 1099 cm^{-1} (O-C-C) their intensity and resolution is lower than those of the NG-PET oligomer whose spectra is undistinguishable from that of PET. We ascribe the difference to the low quantity of grafted oligomer and possibly to its lower crystallinity; the absence of a hydroxyl signal in PET-G is indicative of the reaction of BHET with the oxide as well of the US assisted reduction of the GO.

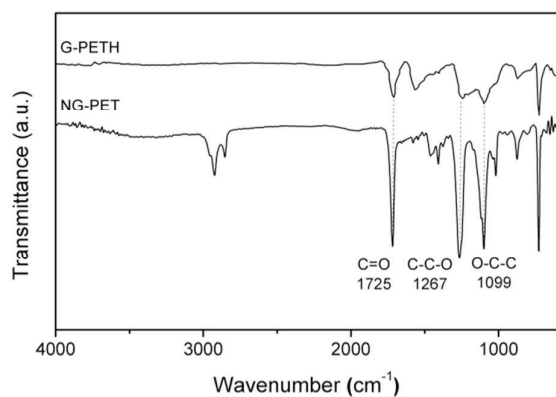


Figure 3. FTIR spectra of NG-PET and PET-G.

Figure 4 shows thermogravimetric analysis of starting GO and graphene grafted PET hybrid nanomaterial (G-PETH). In 4A we observe a 36.8% weight loss of the GO sample at $216.4\text{ }^{\circ}\text{C}$ while G-PETH diminishes its weight in 44.1% at approximately $412.5\text{ }^{\circ}\text{C}$. It is worth noting that no appreciable weight loss around $200\text{ }^{\circ}\text{C}$ related to the removal of GO's oxygen bearing functional groups is observed for the latter. The weight loss at $412.5\text{ }^{\circ}\text{C}$ is associated to the volatilization of PET molecules and is in agreement with the reported degradation temperature of PET/multiwall carbon nanotubes nanocomposites synthesized *in-situ* by Lee *et al* (32). Figure 4B shows the weight loss derivative of both materials showing the typical weight loss of GO slightly above $200\text{ }^{\circ}\text{C}$ at which temperature it decomposes by shedding CO , CO_2 and water. The G-PETH derivative on the other hand shows two signals, a small one centered at $225\text{ }^{\circ}\text{C}$ and a dominant one centered at $412.5\text{ }^{\circ}\text{C}$. The first signal agrees with the decomposition of remaining oxidized groups in the graphitic material while the second corresponds to the previously reported PET decomposition temperature.^{35, 36} The TGA results suggest that some of the oxygen containing GO functional groups reacted with BHET generating PET chains by an US assisted *in-situ* polymerization. The TGA data at $600\text{ }^{\circ}\text{C}$ indicates the carbon content in the PHNCs to be in the proximity of 55.9% by weight.

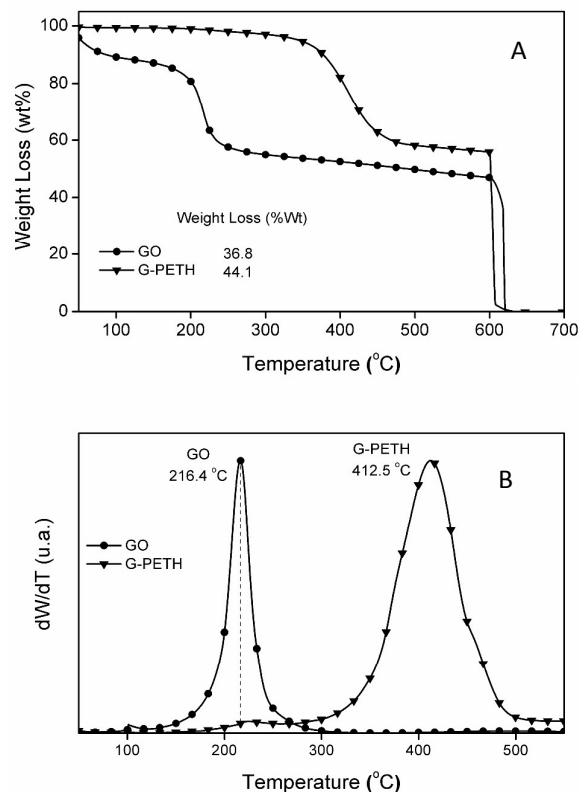


Figure 4. A) Weight loss percentage and B) weight loss derivative of GO and G-PETH obtained by TGA.

To substantiate G-PETH's morphology an X Ray analysis was undertaken, Figure 5 shows the GO and G-PETH corresponding diffractograms. GO shows the expected diffraction of its (001) plane at $2\theta = 11.1\text{ }^{\circ}$ and G-PETH displays an amorphous halo with maximum intensity at $2\theta = 25.2\text{ }^{\circ}$. No GO signal can be seen in nanocomposite's diffractogram, showing GO to have disappeared, either by complete decomposition to graphene or due to their exfoliation in the resulting composite. As no (002) graphite signal can be observed at $2\theta = 26.7\text{ }^{\circ}$, we conclude that is not present or is completely exfoliated within the matrix precluding the formation of stacked graphene layers. The relatively high weight percent of PET contained in the composite, measured by TGA to be 44.1%, is sufficiently high to cover the graphene layers and to prevent their stacking.

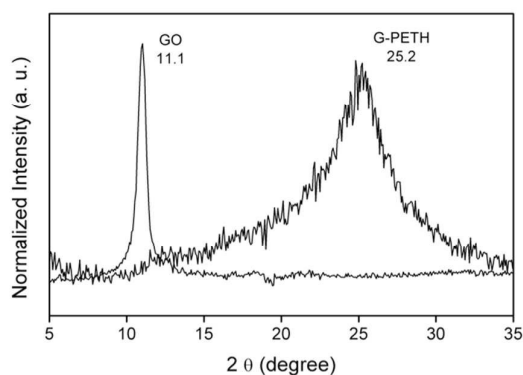


Figure 5. GO and G-PETH X ray diffractograms.

Raman spectroscopic characterization of GO and G-PETH is shown in Figure 6 depicting the D and G bands at approximately 1350 and 1580 cm^{-1} . The bands' position is the same for both compounds and their I_D/I_G intensity ratio is quite similar, of 1.14 for GO and 1.15 in the case of PET, showing that the graphene material does not suffer additional deterioration during the *in-situ* synthesis of hybrid material aid by ultrasound. i.e. the original density of defects presented by the GO remain after the synthesis of G-PETH. It also suggests the persistence of most of the original sp^3 GO, an expected result if the functionalization achieved stems from the grafting of BHET to sp^3 oxygen bearing carbon atoms.

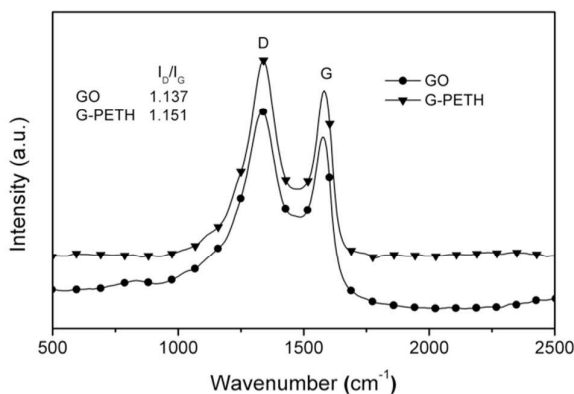


Figure 6. GO and PET-G Raman spectra.

To determine the possible grafting of polymer to the starting GO, we obtained images by TEM. In Figures 7A and 7B the micrographs of GO shows a several-layer material with 2.17 by 1.56 micron dimensions, the phase contrasts and morphology demonstrate the material to be formed of several layers with typical graphene oxide morphology. By comparison 7C and 7D images show that while the material presents a contour typically found in graphene derivatives, the layer thickness is substantially larger than that of GO to the extent of showing

darker areas that inhibit the ease of transmission of the electron's beam. Similar results were observed by examining different sample areas; furthermore no images associated with interlaminar layer separation could be seen. To confirm the material's exfoliation in G-PETH the composite was analyzed by a FE-SEM, in the images of Figure 8 there is no evidence of the typical GO or graphene layer stacking, an observation that further corroborates the layers to be separated as determined by XRD.

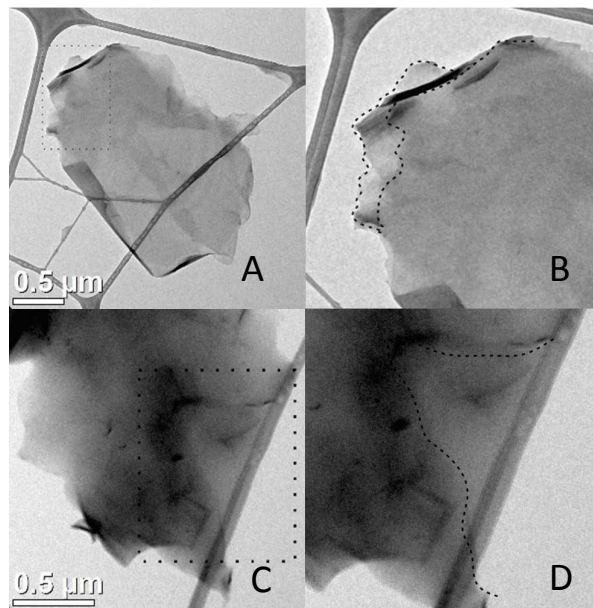


Figure 7. TEM micrographs of the GO and G-PETH's.

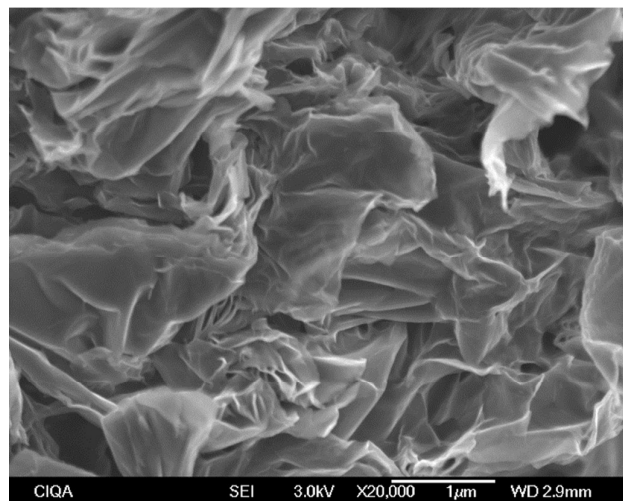


Figure 8. FE-SEM image of G-PETH sample.

ARTICLE

Journal Name

Surface morphology characterization of the GO and G-PETH samples by AFM show in Figure 9 and Figure 10 respectively. The images obtained reveals the typical flakes shape of GO (fig 9 up), the profile section characterization (fig 9 down) ratify that the material was formed of several layers. In the profile section were possible identify at least three steps with different thickness, between 0.98 – 3.08 nm, these values are representative of 3, 5 and 10 GO layers. In case of the G-PETH hybrid nanocomposite, the AFM images show evidence the grafting of polymer to the graphene layers, as showed morphology images and section profiles Figures 10 (up) and 10 (down). The morphological image shows a surface roughness (R_q) of $\approx 1.0 \pm 0.05$ nm. In the profile section was possible identify a 3.9 nm step. The enhanced thickness in the graphene-PET flakes could be related with the polymer grafting due the layer thickness is substantially larger than that of GO sample.

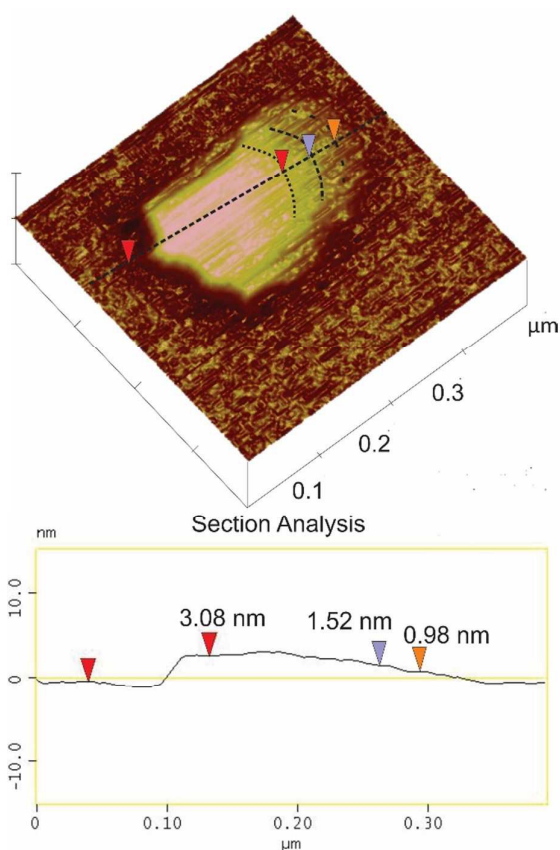


Figure 9: (up) side view of the morphology image (3D) obtained from GO sample, (down) section profile studies in the GO surface.

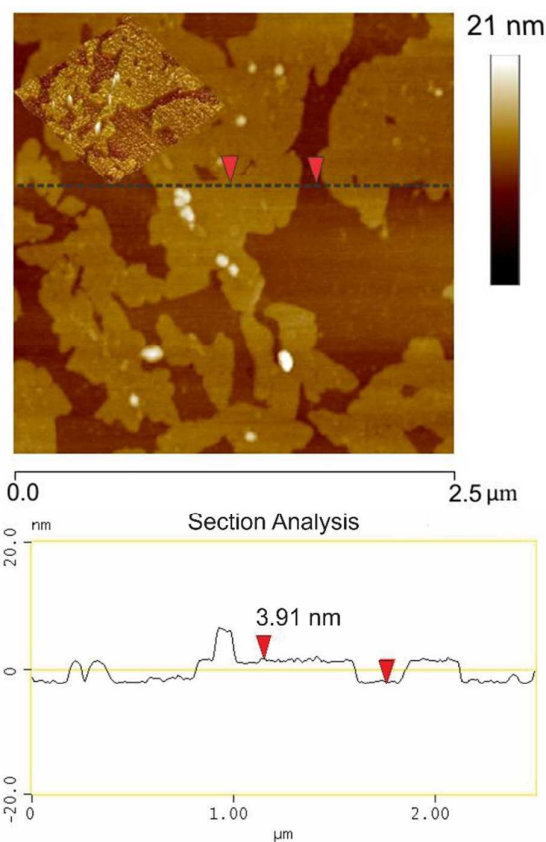


Figure 10: (up) morphology image from G-PETH composite, the inset show a side view (3D) of the surface, (down) section profile studies in the G-PETH composite surface.

Conclusions

PET-Graphene was easily obtained by an ultrasound assisted in-situ polymerization of BHET in the presence of graphite oxide. During the PET grafting from GO synthesis hybridization and exfoliation of the oxide is accomplished in one step. Up to 44% in weight of graphene is grafted to PET oligomers that completely cover the graphene layers. This novel procedure represents a simple and efficient methodology to obtain polymer nanocomposites in which the imbedded graphene is completely exfoliated. It is expected that the oligomer-covered graphene will be highly compatible with virgin polyester resin, easily dispersing in the PET matrix and transferring to it some of the remarkable properties of graphene.

Acknowledgements

The authors thankfully acknowledge Conacyt's funding through the project 250848 "Laboratorio Nacional de Materiales Gráficos". They also thank the technical support of Guadalupe Méndez, Silvia Torres and Enrique Díaz for

carrying out some of the characterization studies reported herein.

Notes and references

1. A. A. Balandin, S. Ghosh, W. Bao, I. Calizo, D. Teweldebrhan, F. Miao and C. N. Lau, *Nano Letters*, 2008, **8**, 902-907.
2. C. Lee, X. Wei, J. W. Kysar and J. Hone, *Science*, 2008, **321**, 385-388.
3. J. Zhu, M. Chen, Q. He, L. Shao, S. Wei and Z. Guo, *RSC Advances*, 2013, **3**, 22790-22824.
4. Q. Bao, H. Zhang, J.-x. Yang, S. Wang, D. Y. Tang, R. Jose, S. Ramakrishna, C. T. Lim and K. P. Loh, *Advanced Functional Materials*, 2010, **20**, 782-791.
5. L. Al-Mashat, K. Shin, K. Kalantar-zadeh, J. D. Plessis, S. H. Han, R. W. Kojima, R. B. Kaner, D. Li, X. Gou, S. J. Ippolito and W. Wlodarski, *The Journal of Physical Chemistry C*, 2010, **114**, 16168-16173.
6. X. Ma, H. Tao, K. Yang, L. Feng, L. Cheng, X. Shi, Y. Li, L. Guo and Z. Liu, *Nano Res.*, 2012, **5**, 199-212.
7. H. Gómez, M. K. Ram, F. Alvi, P. Villalba, E. Stefanakos and A. Kumar, *Journal of Power Sources*, 2011, **196**, 4102-4108.
8. D. Galpaya, M. Wang, M. Liu, N. Motta, E. Waclawik and C. Yan, *Graphene*, 2012, **01**, 21.
9. Z. Song, T. Xu, M. L. Gordin, Y.-B. Jiang, I.-T. Bae, Q. Xiao, H. Zhan, J. Liu and D. Wang, *Nano Letters*, 2012, **12**, 2205-2211.
10. S. Barus, M. Zanetti, M. Lazzari and L. Costa, *Polymer*, 2009, **50**, 2595-2600.
11. X. Cheng, V. Kumar, T. Yokozeki, T. Goto, T. Takahashi, J. Koyanagi, L. Wu and R. Wang, *Composites Part A: Applied Science and Manufacturing*, 2016, **82**, 100-107.
12. J. V. Alemán, A. V. Chadwick, J. He, M. Hess, K. Horie, R. G. Jones, P. Kratochvíl, I. Meisel, I. Mita, G. Moad, S. Penczek and R. F. T. Stepto, in *Pure and Applied Chemistry*, 2007, vol. 79, p. 1801.
13. M. Cano, U. Khan, T. Sainsbury, A. O'Neill, Z. Wang, I. T. McGovern, W. K. Maser, A. M. Benito and J. N. Coleman, *Carbon*, 2013, **52**, 363-371.
14. M. Fang, K. Wang, H. Lu, Y. Yang and S. Nutt, *Journal of Materials Chemistry*, 2009, **19**, 7098-7105.
15. H. He and C. Gao, *Chemistry of Materials*, 2010, **22**, 5054-5064.
16. X. Yan, J. Chen, J. Yang, Q. Xue and P. Miele, *ACS Applied Materials & Interfaces*, 2010, **2**, 2521-2529.
17. M. Kakran, N. G. Sahoo, H. Bao, Y. Pan and L. Li, *Current Medicinal Chemistry*, 2011, **18**, 4503-4512.
18. R. K. Layek and A. K. Nandi, *Polymer*, 2013, **54**, 5087-5103.
19. L. M. Veca, F. Lu, M. J. Meziani, L. Cao, P. Zhang, G. Qi, L. Qu, M. Shrestha and Y.-P. Sun, *Chemical Communications*, 2009, 2565-2567.
20. Y. Lin, J. Jin and M. Song, *Journal of Materials Chemistry*, 2011, **21**, 3455-3461.
21. Y. Li, X. Li, C. Dong, J. Qi and X. Han, *Carbon*, 2010, **48**, 3427-3433.
22. B. Zhang, Y. Chen, L. Xu, L. Zeng, Y. He, E.-T. Kang and J. Zhang, *Journal of Polymer Science Part A: Polymer Chemistry*, 2011, **49**, 2043-2050.
23. T. T. Tung, T. Y. Kim, J. P. Shim, W. S. Yang, H. Kim and K. S. Suh, *Organic Electronics*, 2011, **12**, 2215-2224.
24. L. Valentini, M. Cardinali, S. Bittolo Bon, D. Bagnis, R. Verdejo, M. A. Lopez-Manchado and J. M. Kenny, *Journal of Materials Chemistry*, 2010, **20**, 995-1000.
25. B. Yu, X. Wang, W. Xing, H. Yang, L. Song and Y. Hu, *Industrial & Engineering Chemistry Research*, 2012, **51**, 14629-14636.
26. X. Wang, W. Xing, L. Song, B. Yu, Y. Hu and G. H. Yeoh, *Reactive and Functional Polymers*, 2013, **73**, 854-858.
27. S.-D. Jiang, Z.-M. Bai, G. Tang, Y. Hu and L. Song, *Composites Science and Technology*, 2014, **102**, 51-58.
28. M. Mazloom, M. Rafizadeh, V. Haddadi-Asl and M. Pakniat, *Iranian Polymer Journal*, 2007, **16**, 587-596.
29. H. Patel, G. Feix and R. Schomäcker, *Macromolecular Reaction Engineering*, 2007, **1**, 502-512.
30. J. Chen, B. Yao, C. Li and G. Shi, *Carbon*, 2013, **64**, 225-229.
31. S. K. Srivastava and J. Pionteck, *Journal of Nanoscience and Nanotechnology*, 2015, **15**, 1984-2000.
32. H.-M. Ju, S.-H. Choi and S.-H. Huh, *Journal of the Korean Physical Society*, 2010, **57**, 1649-1652.
33. N. S. Murthy, S. T. Correale and H. Minor, *Macromolecules*, 1991, **24**, 1185-1189.
34. A. Ajji, K. C. Cole, M. M. Dumoulin and J. Brisson, *Polymer*, 1995, **36**, 4023-4030.
35. H.-J. Lee, S.-J. Oh, J.-Y. Choi, J. W. Kim, J. Han, L.-S. Tan and J.-B. Baek, *Chemistry of Materials*, 2005, **17**, 5057-5064.
36. M. C. Costache, M. J. Heidecker, E. Manias and C. A. Wilkie, *Polymers for Advanced Technologies*, 2006, **17**, 764-771.